

Exploring dynamic localization with a Bose-Einstein condensate

André Eckardt¹ and Martin Holthaus²

¹*ICFO-Institut de Ciències Fotòniques, E-08860 Castelldefels (Barcelona), Spain and*

²*Institut für Physik, Carl von Ossietzky Universität, D-26111 Oldenburg, Germany*

Hans Lignier^{3,4}, Alessandro Zenesini^{3,5}, Donatella Ciampini^{3,5}, Oliver Morsch^{3,4}, and Ennio Arimondo^{3,4,5}

³*Dipartimento di Fisica “E. Fermi”, Università di Pisa, Largo Pontecorvo 3, 56127 Pisa, Italy*

⁴*CNR-INFM, Largo Pontecorvo 3, 56127 Pisa, Italy and*

⁵*CNISM UdR Università di Pisa, Largo Pontecorvo 3, 56127 Pisa, Italy*

(Dated: December 1, 2008)

We report on the experimental observation of dynamic localization of a Bose-Einstein condensate in a shaken optical lattice, both for sinusoidal and square-wave forcing. The formulation of this effect in terms of a quasienergy band collapse, backed by the excellent agreement of the observed collapse points with the theoretical predictions, suggests the feasibility of systematic quasienergy band engineering.

PACS numbers: 03.65.Xp, 03.75.Lm, 67.85.Hj

I. INTRODUCTION

The seminal work by Dunlap and Kenkre [1] has led to the recognition that an external uniform ac force can control the spreading of the wave packet of a particle moving in a spatially periodic potential. In particular, an initially localized wave packet of a monochromatically driven particle on a nearest-neighbor tight-binding lattice remains perpetually localized for certain values of the driving amplitude [1]. This phenomenon, termed “dynamic localization”, is a quantum mechanical manifestation of the fact that a time-periodic force sometimes can stabilize a system, as shown in classical mechanics by the example of the driven, inverted pendulum [2]. Dynamic localization is closely related to the coherent destruction of tunneling experienced by a single particle in a double-well potential under the influence of an ac force [3, 4, 5, 6], and to the modification of atomic g -factors in oscillating magnetic fields [7, 8]. In view of possible applications to electrons in terahertz-driven semiconductor superlattices, it has been shown theoretically that dynamic localization survives in the presence of Coulomb interactions [9]. However, experiments with such devices are difficult to perform, and have to cope with a host of competing effects [10]. While there exist clean visualizations of dynamic localization in optical analogs of driven quantum systems, realized by means of curved waveguide arrays for light [11, 12], the observation of dynamic localization of matter waves has long remained a challenge.

The situation changed with the availability of ultracold atoms in optical potentials. In 1998 Madison *et al.* obtained evidence for band narrowing with cold sodium atoms in a phase-modulated optical lattice, in good agreement with theoretical calculations going beyond both the tight-binding and the single-band approximation [13]. More recently, the basic mechanism responsible for dynamic localization, an effective rescaling of the hopping matrix element induced by the ac force, has been

observed for single-particle tunneling in strongly driven double-well potentials [14]. It had also been pointed out that this mechanism remains effective even for an interacting Bose-Einstein condensate, at least for sufficiently high driving frequencies [15]. This has led to the experimental demonstration of dynamic control of matter-wave tunneling in an optical lattice [16], and to the observation of photon-assisted tunneling of a condensate [17]. Since the reduction of interwell tunneling increases the relative importance of the particles’ repulsion, even the superfluid-to-Mott insulator transition of ultracold atoms in an optical lattice can be induced by shaking the lattice in a time-periodic manner, as has now been shown by Zenesini *et al.* [18]

In the present paper we take up this line of investigation and explore dynamic localization of a dilute Bose-Einstein condensate in a time-periodically shifted optical lattice in more detail. We proceed as follows: In Sec. II we cast the concept of single-particle dynamic localization into a form that lends itself in a particularly transparent manner to further generalizations, relying on the idea of quasienergy bands [19]. We then apply these general considerations in Sec. III to optical cosine lattices, taking into account all couplings that are omitted in the nearest-neighbor approximation. In Sec. IV we report our experimental results, achieved with condensates of ⁸⁷Rb. Besides sinusoidal forcing, we also consider the case of square-wave forcing, which is known to produce exact single-particle dynamic localization for any form of the energy dispersion [20, 21]. The final Sec. V contains our conclusions.

II. THE PRINCIPLE UNDERLYING DYNAMIC LOCALIZATION

We consider a time-dependent Hamiltonian

$$H(t) = H_0 + H_1(t), \quad (1)$$

where

$$H_0 = \frac{p^2}{2m} + V(x) \quad (2)$$

describes a single particle with mass m moving in a one-dimensional periodic potential $V(x) = V(x + d)$ with lattice constant d , and

$$H_1(t) = -F(t)x \quad (3)$$

introduces an external force $F(t)$, mediated by the position operator x in a manner analogous to electromagnetic forces on atoms within the dipole approximation. The energy eigenfunctions $\varphi_{n,k}(x)$ of H_0 are Bloch states with band index n and wave number k ,

$$\varphi_{n,k}(x) = e^{ikx}v_{n,k}(x), \quad (4)$$

with functions $v_{n,k}(x) = v_{n,k}(x + d)$ sharing the spatial lattice period d . The solutions to the eigenvalue equation

$$H_0\varphi_{n,k}(x) = E_n(k)\varphi_{n,k}(x) \quad (5)$$

provide the dispersion relations $E_n(k)$ for the various energy bands. It is of interest to observe that the external forcing does not truly break translational symmetry: Introducing the unitary transformation

$$U = \exp\left(-\frac{i}{\hbar} \int_{t_0}^t d\tau F(\tau)x\right), \quad (6)$$

the transformed wave functions $\tilde{\psi}(x, t) = U\psi(x, t)$ are governed by the Hamiltonian

$$\tilde{H}(t) = \frac{1}{2m} \left(p + \int_{t_0}^t d\tau F(\tau)\right)^2 + V(x), \quad (7)$$

which still remains invariant under spatial translations by d .

In the following, we assume band gaps so wide that, despite the external force, the dynamics can be restricted to the lowest band. Dropping the band index, we expand the Bloch waves of that band with respect to the corresponding Wannier states [22, 23],

$$\varphi_k(x) = \sum_{\ell} w_{\ell}(x)e^{ik\ell d}, \quad (8)$$

where $w_{\ell}(x) = w_0(x - \ell d)$ denotes a Wannier function centered around the ℓ -th lattice site. We take the potential to be symmetric, $V(x) = V(-x)$, so that $w_0(x)$ can be chosen real and symmetric [23]. Defining the time-dependent wave number

$$q_k(t) = k + \frac{1}{\hbar} \int_{t_0}^t d\tau F(\tau), \quad (9)$$

obeying $\hbar\dot{q}_k(t) = F(t)$ and containing a still unspecified lower integration bound t_0 , the wave functions

$$\psi_k(x, t) = \sum_{\ell} w_{\ell}(x)e^{iq_k(t)\ell d} \exp\left(-\frac{i}{\hbar} \int_0^t d\tau E(q_k(\tau))\right) \quad (10)$$

then are ‘‘weak’’ solutions to the time-dependent Schrödinger equation with the full Hamiltonian (1), in the following sense: By construction, one has

$$\begin{aligned} i\hbar \frac{\partial}{\partial t} \psi_k(x, t) &= E(q_k(t))\psi_k(t) \\ -F(t) \sum_{\ell} \ell d w_{\ell}(x) e^{iq_k(t)\ell d} \exp\left(-\frac{i}{\hbar} \int_0^t d\tau E(q_k(\tau))\right). \end{aligned} \quad (11)$$

If we stipulate that the lattice site labeled $\ell = 0$ is situated at $x = 0$, implying

$$\langle 0 | x | 0 \rangle = \int dx x |w_0(x)|^2 = 0, \quad (12)$$

then one has

$$\langle \ell | x | m \rangle = \begin{cases} \ell d, & \text{if } \ell = m \\ 0, & \text{else} \end{cases}, \quad (13)$$

where $|\ell\rangle$ is the Dirac ket corresponding to $w_{\ell}(x)$. Note that this is an identity, which holds exactly even for shallow lattices. Hence, it follows that

$$\begin{aligned} \langle \ell | i\hbar \frac{\partial}{\partial t} \psi_k(x, t) \rangle &= \langle \ell | E(q_k(t)) - F(t)x | \psi_k(x, t) \rangle \\ &= \langle \ell | H_0 + H_1(t) | \psi_k(x, t) \rangle \end{aligned} \quad (14)$$

for each ℓ .

The above wave functions (10) can be regarded as Houston states [24], also known as ‘‘accelerated Bloch states’’, and apply to any type of uniform forcing $F(t)$, provided the single-band approximation remains viable. If we now require that the forcing be periodic with period T and zero average, so that $F(t) = F(t + T)$ and

$$\frac{1}{T} \int_0^T dt F(t) = 0, \quad (15)$$

a further step can be made: In this case the transformed Hamiltonian (7) is periodic in both space and time, thus giving rise to spatio-temporal Bloch waves

$$\tilde{\psi}_k(x, t) = \tilde{v}_k(x, t) \exp(ikx - i\varepsilon(k)t/\hbar) \quad (16)$$

with quasimomenta $\hbar k$, quasienergies $\varepsilon(k)$, and time-dependent Bloch functions obeying $\tilde{v}(x, t) = \tilde{v}(x + d, t) = \tilde{v}(x, t + T)$.

When deriving these states within the single-band approximation from the Houston states (10), a slight subtlety comes into play: The lower integration bound t_0 in the definition (9) of $q_k(t)$ effectuates a shift of the wave number k . In order to avoid this shift, and thus to make sure that the wave number k labeling a spatio-temporal Bloch wave is the same as the one which labels the Bloch state continuously connected to it when the driving force vanishes, this lower bound t_0 has to be chosen such that the integrated force also has zero average, requiring

$$\frac{1}{T} \int_0^T dt \int_{t_0}^t d\tau F(\tau) = 0. \quad (17)$$

With this specification of $q_k(t)$, we set

$$\varepsilon(k) = \frac{1}{T} \int_0^T dt E(q_k(t)), \quad (18)$$

and write the Houston states (10) in the form

$$\psi_k(x, t) = u_k(x, t) \exp\left(-\frac{i}{\hbar} \varepsilon(k)t\right). \quad (19)$$

This formal-looking manipulation is of key significance: After the average phase growth has been factored out, the remaining functions $u_k(x, t)$ acquire the temporal periodicity of the force,

$$\begin{aligned} u_k(x, t) &= \sum_{\ell} w_{\ell}(x) e^{iq_k(t)\ell d} \\ &\times \exp\left(-\frac{i}{\hbar} \int_0^t d\tau \left(E(q_k(\tau)) - \varepsilon(k)\right)\right) \\ &= u_k(x, t + T). \end{aligned} \quad (20)$$

Thus, these wave functions (19) are Floquet states [8, 19], from which the spatio-temporal Bloch waves (16) are obtained by applying the unitary transformation (6). At times $t = t_0 + sT$ (with integer s) they coincide with the Bloch waves (8), apart from a phase factor. *Any* single-band wave packet $\psi(x, t)$ can be expanded with respect to these basis states,

$$\psi(x, t) = \left(\frac{d}{2\pi}\right)^{1/2} \int_{-\pi/d}^{\pi/d} dk a(k) u_k(x, t) \exp\left(-\frac{i}{\hbar} \varepsilon(k)t\right), \quad (21)$$

with some density $a(k)$ which is time-independent despite the presence of the ac force. The T -periodic nature of the functions $u_k(x, t)$ directly reflects the short-term response of such a packet to the force $F(t)$, whereas the quasienergy dispersion $\varepsilon(k)$ governs its long-time averaged evolution in the same manner as the original energy dispersion $E(k)$ governs its evolution when $F(t) = 0$. For example, the average velocity \bar{v}_{k_0} of a wave packet initially centered around some wave number k_0 is given, in the presence of the forcing, by

$$\bar{v}_{k_0} = \frac{1}{\hbar} \left. \frac{\partial \varepsilon(k)}{\partial k} \right|_{k=k_0}. \quad (22)$$

Moreover, the representation (21) directly leads to a quite general and intuitive condition for dynamic localization: Exact dynamic localization obviously occurs when the quasienergy band collapses, so that all quasienergies coincide, $\varepsilon(k) = \varepsilon_0$ for all k , implying that the effective mass of a driven Bloch particle becomes infinite. All Floquet states comprising the wave packet (21) then acquire exactly the same phase in the course of one driving period, since

$$\psi(x, t) = \exp\left(-\frac{i}{\hbar} \varepsilon_0 t\right) \left(\frac{d}{2\pi}\right)^{1/2} \int_{-\pi/d}^{\pi/d} dk a(k) u_k(x, t), \quad (23)$$

V_0/E_r	c_1	c_2	c_3	c_4
2.0	-0.14276	$2.04 \cdot 10^{-2}$	$-4.83 \cdot 10^{-3}$	$1.40 \cdot 10^{-3}$
4.0	-0.08549	$6.15 \cdot 10^{-3}$	$-7.16 \cdot 10^{-4}$	$1.01 \cdot 10^{-4}$
6.0	-0.05077	$1.91 \cdot 10^{-3}$	$-1.15 \cdot 10^{-4}$	$8.31 \cdot 10^{-6}$
8.0	-0.03080	$6.35 \cdot 10^{-4}$	$-2.08 \cdot 10^{-5}$	$8.20 \cdot 10^{-7}$
10.0	-0.01918	$2.27 \cdot 10^{-4}$	$-4.25 \cdot 10^{-6}$	$9.57 \cdot 10^{-8}$
12.0	-0.01225	$8.66 \cdot 10^{-5}$	$-9.65 \cdot 10^{-7}$	$1.29 \cdot 10^{-8}$
14.0	-0.00800	$3.49 \cdot 10^{-5}$	$-2.39 \cdot 10^{-7}$	$1.96 \cdot 10^{-9}$
16.0	-0.00533	$1.47 \cdot 10^{-5}$	$-6.37 \cdot 10^{-8}$	$3.31 \cdot 10^{-10}$
18.0	-0.00362	$6.48 \cdot 10^{-6}$	$-1.81 \cdot 10^{-8}$	$6.09 \cdot 10^{-11}$
20.0	-0.00249	$2.95 \cdot 10^{-6}$	$-5.45 \cdot 10^{-9}$	$1.22 \cdot 10^{-11}$

TABLE I: Hopping matrix elements $c_{\ell} = \langle 0|H_0|\ell\rangle/E_r$ for the lowest band of an optical cosine lattice (25), as functions of the scaled lattice depth V_0/E_r . Observe that the sign of c_{ℓ} alternates with ℓ .

so that the packet can neither move (apart from its residual T -periodic motion) nor spread, but simply reproduces itself T -periodically, regardless of the form of the density $a(k)$. When this condition of zero width of the quasienergy band cannot be met exactly, but there still is significant band narrowing, wave packet spreading can at least be reduced substantially by the external force [19].

III. APPLICATION TO OPTICAL LATTICES

For a lattice with inversion symmetry, the original energy dispersion takes the form

$$E(k) = E_0 + \sum_{\ell=1}^{\infty} 2\langle 0|H_0|\ell\rangle \cos(\ell kd), \quad (24)$$

with coefficients given by matrix elements of H_0 between Wannier states located ℓ sites apart from each other. In particular, for an optical cosine lattice of the form [25]

$$V(x) = \frac{V_0}{2} \cos(2k_L x), \quad (25)$$

where k_L is the wave number of the lattice-generating laser radiation and the depth V_0 is proportional to the intensity of that radiation [25], the Wannier states can easily be computed numerically [26, 27]. Table I lists the resulting coupling coefficients $\langle 0|H_0|\ell\rangle$ for the lowest band as functions of the scaled lattice depth V_0/E_r , with

$$E_r = \frac{\hbar^2 k_L^2}{2m} \quad (26)$$

denoting the single-photon recoil energy of an atom with mass m . The relative error committed when adopting the commonly used nearest-neighbor approximation, *i.e.*, when neglecting all $\langle 0|H_0|\ell\rangle$ with $\ell \geq 2$, is on the order of 10% for an optical lattice with $V_0/E_r = 3$, and reduces to 1% only when $V_0/E_r \approx 10$ [27].

A. Sinusoidal forcing

We now consider purely sinusoidal forcing, as specified by $F(t) = F_0 \cos(\omega t + \varphi)$ with some arbitrary phase φ . In this case, Eq. (9) together with the requirement (17) yields

$$q_k(t) = k + \frac{F_0}{\hbar\omega} \sin(\omega t + \varphi), \quad (27)$$

implying

$$\frac{1}{T} \int_0^T dt \cos(q_k(t)\ell d) = J_0(\ell K_0) \cos(\ell k d), \quad (28)$$

where $J_0(z)$ is a Bessel function of order zero, and we have introduced the scaled driving amplitude

$$K_0 = \frac{F_0 d}{\hbar\omega}. \quad (29)$$

Hence, the quasienergy dispersion resulting from the Bloch band (24) under sinusoidal forcing reads

$$\varepsilon(k) = E_0 + \sum_{\ell=1}^{\infty} 2\langle 0|H_0|\ell\rangle J_0(\ell K_0) \cos(\ell k d). \quad (30)$$

For the particular example of quasienergy bands originating from the lowest Bloch band of an optical lattice (25), characterized by the matrix elements collected in Table I, the quasienergy band widths are depicted in Fig. 1 as functions of K_0 for some typical depths V_0 . Due to the dominance of the nearest-neighbor hopping matrix element $\langle 0|H_0|1\rangle$ there is strong band narrowing for values of K_0 close to the zeros of the Bessel function J_0 , but the nonvanishing longer-range hopping elements prevent the band from collapsing completely, as emphasized by the inset. Thus, one expects appreciable, but incomplete dynamic localization in sinusoidally driven shallow optical lattices.

B. Square-wave forcing

For square-wave forcing of the form

$$F(t) = \begin{cases} F_0 & , \quad 0 \leq t < T/2 \\ -F_0 & , \quad T/2 \leq t < T \end{cases}, \quad (31)$$

Eqs. (9) and (17) yield

$$q_k(t) = \begin{cases} k + F_0(t - T/4)/\hbar & , \quad 0 \leq t < T/2 \\ k + F_0(3T/4 - t)/\hbar & , \quad T/2 \leq t < T \end{cases}, \quad (32)$$

to be continued T -periodically to all t . This gives

$$\frac{1}{T} \int_0^T dt \cos(q_k(t)\ell d) = \text{sinc}\left(\frac{\ell\pi K_0}{2}\right) \cos(\ell k d), \quad (33)$$

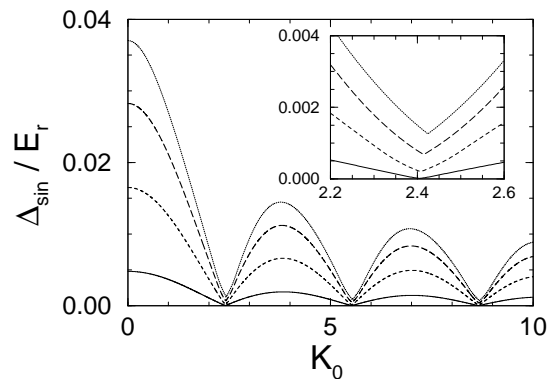


FIG. 1: Width Δ_{sin} of the lowest quasienergy band of an optical cosine lattice under sinusoidal driving as function of the dimensionless amplitude (29), for $V_0/E_r = 2$ (dots), 3 (long dashes), 5 (short dashes), and 10 (full line). The inset quantifies the extent of band narrowing for values of K_0 close to the first zero $j_{0,1} = 2.405$ of the Bessel function J_0 .

with K_0 being defined according to Eq. (29), having set $\omega = 2\pi/T$. Moreover, we write $\text{sinc}(z) = \sin(z)/z$. Correspondingly, the quasienergy dispersion becomes

$$\varepsilon(k) = E_0 + \sum_{\ell=1}^{\infty} 2\langle 0|H_0|\ell\rangle \text{sinc}\left(\frac{\ell\pi K_0}{2}\right) \cos(\ell k d). \quad (34)$$

Since all sinc-functions adopt their zeros simultaneously, there is a total collapse of this quasienergy band when $K_0 = 2\nu$ with integer $\nu = 1, 2, 3, \dots$. Thus, we recover the known fact that there is exact dynamic localization, regardless of both the values of the hopping matrix elements and the form of the wave packet, for these particular driving amplitudes [20, 21]. Figure 2 shows the widths of quasienergy bands originating from the lowest Bloch band of an optical lattice under square-wave forcing; the total band collapse at $K_0 = 2$ is clearly visible in the inset.

IV. EXPERIMENTAL RESULTS

Our experimental setup is described in detail in Ref. [16]. Briefly, we adiabatically load Bose-Einstein condensates consisting of about 6×10^4 atoms of ^{87}Rb into the lowest band of a one-dimensional optical lattice. The lattice is generated by focusing two counter-propagating linearly polarized laser beams of wavelength $\lambda = 2\pi/k_L = 842$ nm onto the condensate, resulting in the periodic potential (25) along the beam direction. Each beam passes through an acousto-optic modulator, allowing us to introduce a frequency difference $\Delta\nu(t)$ between the beams that can be used to accelerate or shake the lattice. In the laboratory frame of reference, the condensate then experiences a time-dependent potential

$$V_{\text{lab}}(x, t) = \frac{V_0}{2} \cos\left(2k_L \left[x - \frac{\lambda}{2} \int_{t_1}^t d\tau \Delta\nu(\tau)\right]\right). \quad (35)$$

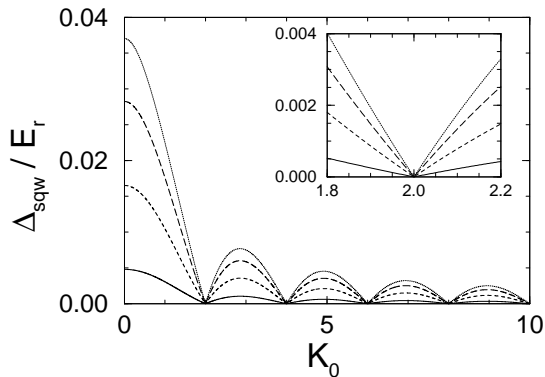


FIG. 2: Width Δ_{sqw} of the lowest quasienergy band of an optical cosine lattice under square-wave driving as function of the dimensionless amplitude (29), for $V_0/E_r = 2$ (dots), 3 (long dashes), 5 (short dashes), and 10 (full line). The inset illustrates that an exact band collapse occurs when K_0 is a nonzero integer multiple of 2.

By means of a unitary transformation to the comoving frame of reference, the single-particle Hamiltonian is brought into the form

$$H = \frac{p^2}{2m} + \frac{V_0}{2} \cos(2k_L x) + m \frac{\lambda}{2} \frac{d\Delta\nu(t)}{dt} x. \quad (36)$$

Hence, prescribing an oscillating frequency difference

$$\Delta\nu(t) = \Delta\nu_{\text{max}} \sin(\omega t) \quad (37)$$

with amplitude $\Delta\nu_{\text{max}}$, one obtains sinusoidal forcing with strength $F_0 = m\omega\lambda\Delta\nu_{\text{max}}/2$, amounting to the scaled driving amplitude

$$K_0 = \frac{\pi^2}{2} \frac{\hbar\Delta\nu_{\text{max}}}{E_r}. \quad (38)$$

On the other hand, the triangular protocol

$$\Delta\nu(t) = \begin{cases} 2\Delta\nu_{\text{max}}t/T & , \quad 0 \leq t < T/2 \\ 2\Delta\nu_{\text{max}}(1-t/T) & , \quad T/2 \leq t < T \end{cases} \quad (39)$$

results in square-wave forcing with strength $F_0 = m\lambda\Delta\nu_{\text{max}}/T$, giving

$$K_0 = \frac{\pi}{2} \frac{\hbar\Delta\nu_{\text{max}}}{E_r}. \quad (40)$$

We first study the *in situ* expansion of a condensate under both kinds of forcing [16]. To this end, initially an anisotropic, elongated harmonic trap with trapping frequencies of 20 Hz (longitudinally) and 80 Hz (radially) was superimposed on the lattice. After switching off the laser beam effectuating the longitudinal confinement, the condensate was free to expand in the direction of the shaken lattice. After some time, it was illuminated by a resonant flash, the shadow cast by which was imaged onto a CCD chip.

We work with lattices possessing a fairly large depth between $V_0 = 6E_r$ and $V_0 = 9E_r$, so that the effect of longer-range hopping is not discernible at the scale of our experimental accuracy, and we may employ the nearest-neighbor approximation, keeping only the hopping matrix element $J = -\langle 0|H_0|1\rangle$ connecting adjacent lattice sites. Thus, the unperturbed energy band is well described by the cosine dispersion relation

$$E(k) = -2J \cos(kd), \quad (41)$$

assuming that interparticle interactions remain negligible. Accordingly, the quasienergy band of the driven system is approximated by

$$\varepsilon(k) = -2J_{\text{eff}} \cos(kd), \quad (42)$$

where the effective hopping matrix element J_{eff} is given by

$$J_{\text{eff}} = J J_0(K_0) \quad (43)$$

for sinusoidal forcing, as follows from Eq. (30), whereas Eq. (34) gives

$$J_{\text{eff}} = J \text{sinc}(\pi K_0/2) \quad (44)$$

for a square-wave drive. The measured expansion rate $d\sigma_x/dt$ of the condensate width σ_x along the lattice direction is then to a good approximation proportional to the hopping element J_{eff} which effectively describes nearest-neighbor tunneling when the forcing is present [16]. This is a working example of our general philosophy: The time-averaged evolution of the driven system proceeds in close analogy to that of an undriven one, with $\varepsilon(k)$ replacing $E(k)$. In practice, rather than extracting J_{eff} from the expansion data, for each experiment we also measure the bare expansion rate (which is proportional to J) in the undriven system, from which the normalized effective hopping element J_{eff}/J is then calculated.

In Fig. 3 we plot our results for both types of forcing versus the scaled driving amplitude K_0 , obtained with a sinusoidal drive of frequency $\omega/2\pi = 1.0$ kHz, and a square-wave one with $\omega/2\pi = 1.5$ kHz. Evidently, the single-particle expectations are matched quite well, with the data obtained for square-wave driving scattering a bit more strongly around the prediction (44) than those for sinusoidal driving around the graph of Eq. (43).

An alternative method for determining the points of maximum band collapse is to measure the phase coherence of the condensate in the shaken lattice [16]. Switching off the confining potential and letting the condensate fall under gravity for 20 ms, we obtain an interference pattern whose visibility reflects the condensate coherence. Recording this visibility as a function of time, we extract the decay time constant τ_{deph} of the resulting near-exponential function. In general, we find dephasing times on the order of 100 ms in the presence of even strong sinusoidal driving, while they are somewhat shorter for the square-wave drive, as shown in Fig. 4. In

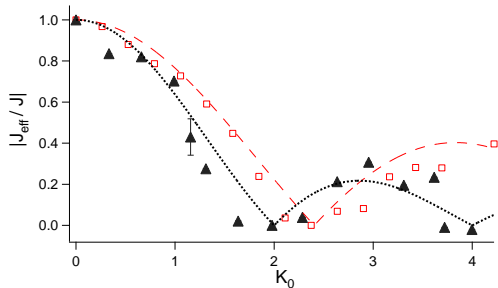


FIG. 3: (Color online) Absolute value of the effective hopping matrix element J_{eff} for a condensate in an optical lattice with depth $V_0/E_r = 6$ under the influence of sinusoidal (open boxes) and square-wave (triangles) driving, normalized to the “bare” hopping element J which governs the condensate spreading in the undriven lattice. The lines correspond to the approximations (43) and (44). The driving frequencies $\omega/2\pi$ were 1.0 kHz for sinusoidal driving, and 1.5 kHz for the square-wave case.

the immediate vicinity of the band collapse points, however, the dephasing times are strongly reduced: When the quasienergy band width approaches zero, the individual lattice sites are effectively decoupled, so that the local phases evolve independently due to interatomic collisions, resulting in a rapid dephasing of the array. This effect leads to sharply pronounced dips in plots of τ_{deph} vs. K_0 , allowing us to confirm the theoretically predicted first collapse points to fairly good accuracy: $K_0 = 2.4$ for sinusoidal forcing, whereas $K_0 = 2.0$ for the square-wave drive.

While in the present work we are mainly concerned with identifying the conditions for partial or complete dynamic localization, useful insight can also be obtained by studying the time evolution of the width of the driven matter-wave packet away from the collapse points. In general, if the extension σ_x of a Floquet wave packet (21) narrowly centered in k -space around some k_0 is given by $\sigma_x = a$ at time $t = 0$, that wave packet spreads in time according to

$$\begin{aligned} \sigma_x(t) &= a \sqrt{1 + \left(\frac{\varepsilon''(k_0)t}{\hbar a^2}\right)^2} \\ &\sim \gamma_a(k_0)t, \end{aligned} \quad (45)$$

with asymptotic, large- t expansion rate

$$\gamma_a(k_0) = \frac{|\varepsilon''(k_0)|}{\hbar a} \quad (46)$$

determined by the second derivative of the quasienergy dispersion at k_0 . According to Eqs. (30) and (34), here the hopping elements $\langle 0|H_0|\ell\rangle$ enter with weights proportional to ℓ^2 , each depending in a different manner on the driving amplitude. Hence, precise measurements of the expansion rate could yield information both on the state of the driven packet, *i.e.*, on the wave number k_0 ,

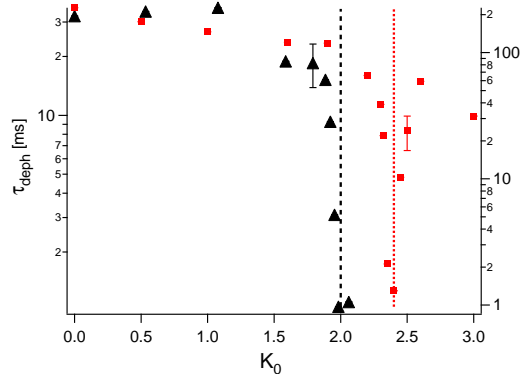


FIG. 4: (Color online) Dephasing times for a condensate in an optical lattice with depth $V_0/E_r = 9$ under the influence of square-wave (triangles; left scale) and sinusoidal (boxes; right scale) driving.

and on the next-to-nearest neighbor couplings. Furthermore, while we have worked with condensate densities so low that interparticle interactions can be ignored and the single-particle picture remains applicable, it would be interesting to identify signatures of interparticle interactions in dynamic localization.

V. CONCLUSIONS AND OUTLOOK

In this work we have pointed out that wave packet motion and spreading in time-periodically forced spatially periodic potentials are governed by quasienergy bands $\varepsilon(k)$ in a manner which exactly parallels the description of quantum dynamics in unforced lattices in terms of their energy bands $E(k)$, and have experimentally demonstrated dynamic localization, *i.e.*, “freezing” of the dynamics due to a quasienergy band collapse, with dilute Bose-Einstein condensates in optical lattices subjected to either sinusoidal or square-wave driving. Seen from a conceptual viewpoint, this experimental confirmation of the ideas developed in the context of dynamic localization can be regarded as a proof of principle for the notion of *quasienergy band engineering*: Different types of forcing, applied to the same energy band, can lead to substantially different quasienergy dispersion relations, and hence can be employed for realizing band structures which even might not have an analog in traditional solid-state systems.

In order to make contact with previous theoretical works [1, 5, 19, 20, 21], we have restricted our investigation here to forces with parameters which do not lead to significant coupling of several energy bands. In this case the construction of the quasienergy dispersion merely involves taking the average (18) and thus is an easy exercise, since one is essentially dealing with just a free Bloch particle. However, such quasienergy bands, reflecting the existence of spatio-temporal Bloch waves (16), originate from nothing more than the simultaneous pres-

ence of a spatially periodic potential and a temporally periodic force. Accordingly, they also exist when several unperturbed energy bands are coupled by the force; the quasienergy bands then exhibit fairly nontrivial features [8]. The exploration of these further options for band engineering which result from deliberate interband coupling, together with the inclusion of interparticle interaction, should open up further interesting avenues.

Acknowledgments

A.E. is grateful to M. Lewenstein for kind hospitality at ICFO-Institut de Ciències Fotòniques, and acknowledges

a Feodor Lynen research grant from the Alexander von Humboldt foundation. Financial support by the E.U.-STREP “OLAQUI” and by a CNISM “Progetto Innesco 2007” for the experimental part of this work is also gratefully acknowledged. We thank J. Radogostowicz, C. Sias and Y. Singh for assistance.

-
- [1] D. H. Dunlap and V. M. Kenkre, *Phys. Rev. B* **34**, 3625 (1986).
- [2] E. I. Butikov, *Am. J. Phys.* **69**, 755 (2001).
- [3] F. Grossmann, T. Dittrich, P. Jung, and P. Hänggi, *Phys. Rev. Lett.* **67**, 516 (1991).
- [4] J. M. Gomez Llorente and J. Plata, *Phys. Rev. A* **45**, R6958 (1992); Erratum: *Phys. Rev. E* **49**, 3547 (1994).
- [5] M. Grifoni and P. Hänggi, *Phys. Rep.* **304**, 229 (1998).
- [6] Y. Kayanuma and K. Saito, *Phys. Rev. A* **77**, 010101(R) (2008).
- [7] S. Haroche, C. Cohen-Tannoudji, C. Audoin, and J. P. Schermann, *Phys. Rev. Lett.* **24**, 861 (1970).
- [8] M. Holthaus and D. W. Hone, *Phil. Mag. B* **74**, 105 (1996).
- [9] T. Meier, G. von Plessen, P. Thomas, and S. W. Koch, *Phys. Rev. B* **51**, 14490 (1995).
- [10] B. J. Keay, S. Zeuner, S. J. Allen, Jr., K. D. Maranowski, A. C. Gossard, U. Bhattacharya, and M. J. W. Rodwell, *Phys. Rev. Lett.* **75**, 4102 (1995).
- [11] S. Longhi, M. Marangoni, M. Lobino, R. Ramponi, P. Laporta, E. Cianci, and V. Foglietti, *Phys. Rev. Lett.* **96**, 243901 (2006).
- [12] G. Della Valle, M. Ornigotti, E. Cianci, V. Foglietti, P. Laporta, and S. Longhi, *Phys. Rev. Lett.* **98**, 263601 (2007).
- [13] K. W. Madison, M. C. Fischer, R. B. Diener, Q. Niu, and M. G. Raizen, *Phys. Rev. Lett.* **81**, 5093 (1998).
- [14] E. Kierig, U. Schnorrberger, A. Schietinger, J. Tomkovic, and M. K. Oberthaler, *Phys. Rev. Lett.* **100**, 190405 (2008).
- [15] A. Eckardt, C. Weiss, and M. Holthaus, *Phys. Rev. Lett.* **95**, 260404 (2005).
- [16] H. Lignier, C. Sias, D. Ciampini, Y. Singh, A. Zenesini, O. Morsch, and E. Arimondo, *Phys. Rev. Lett.* **99**, 220403 (2007).
- [17] C. Sias, H. Lignier, Y. P. Singh, A. Zenesini, D. Ciampini, O. Morsch, and E. Arimondo, *Phys. Rev. Lett.* **100**, 040404 (2008).
- [18] A. Zenesini, H. Lignier, D. Ciampini, O. Morsch, and E. Arimondo, arXiv:0809.0768.
- [19] M. Holthaus and D. Hone, *Phys. Rev. B* **47**, 6499 (1993).
- [20] M. J. Zhu, X.-G. Zhao, and Q. Niu, *J. Phys.: Condens. Matter* **11**, 4527 (1999).
- [21] M. M. Dignam and C. M. de Sterke, *Phys. Rev. Lett.* **88**, 046806 (2002).
- [22] G. H. Wannier, *Phys. Rev.* **52**, 191 (1937).
- [23] W. Kohn, *Phys. Rev.* **115**, 809 (1959).
- [24] W. V. Houston, *Phys. Rev.* **57**, 184 (1940).
- [25] O. Morsch and M. K. Oberthaler, *Rev. Mod. Phys.* **78**, 179 (2006).
- [26] J. C. Slater, *Phys. Rev.* **87**, 807 (1952).
- [27] D. J. Boers, B. Goedeke, D. Hinrichs, and M. Holthaus, *Phys. Rev. A* **75**, 063404 (2007).